Journal of Medicinal and Chemical Sciences 6 (2023) 3087-3112

Journal of Medicinal and Chemical Sciences

Journal homepage: http://www.jmchemsci.com/

Original Article

QSAR Modeling, Molecular Docking, and ADME Studies of Novel 5-Oxo- Imidazoline Derivatives as Anti-Breast Cancer Drug Compounds against MCF-7 Cell Line

Yellasubbaiah N, Velmurugan V*

Department of Pharmaceutical Chemistry, Faculty of Medicine and Health Sciences, SRM Institute of Science and Technology, SRM College of Pharmacy, Kattankulathur – 603203, Chengalpattu District, Tamil Nadu, India

ARTICLE INFO

Article history

Receive: 2023-06-04
Received in revised: 2023-07-28
Accepted: 2023-08-01
Manuscript ID: JMCS-2307-2144
Checked for Plagiarism: **Yes**
Language Editor:
Dr. Fatima Ramezani
Editor who approved publication:
Dr. Ehab Al Shamaileh

DOI:10.26655/JMCHEMSCI.2023.12.24

KEYWORDS

QSAR analysis
5-(mercapto 1, 3, 4-oxadiazole)-5-oxo-imidazolines
Molecular docking studies
Polo-like kinases (plk1) inhibitors
Breast cancer

ABSTRACT

Thirty-six (36) new 5-oxo-imidazoline derivatives were studied using Insilco modeling against MCF-7 breast cancer cell lines. This research included QSAR, molecular docking, and pharmacokinetic analysis of the developed drugs. Based on the numerical evaluation of R^2 = 0.7499, (R^2_{adj}) = 0.7061, (CCC_{ext}) = 0.6877, and (R^2_{ext}) = 0.6726, Model one performed best in the QSAR study. New derivative drugs with improved efficacy against estrogen-positive breast cancer (MCF-7 cell line) were designed using model number one. Derivatives of 5-(mercapto 1, 3, 4-oxadiazole)-5-oxo-imidazolines were predicted to be potent inhibitors of polo-like kinase 1 (plk1) based on molecular docking studies between the derivatives and the plk1 receptor. The results of the pharmacokinetic analysis of the new structures showed that they all met the criteria, including the Lipinski Rule of Five, and could move on to pre-clinical testing. They both showed that the MCF-7 cell line might be a unique therapeutic target in the fight against breast cancer.

* Corresponding author: Velmurugan V
✉ E-mail: velmuruv@srmist.edu.in

GRAPHICAL ABSTRACT

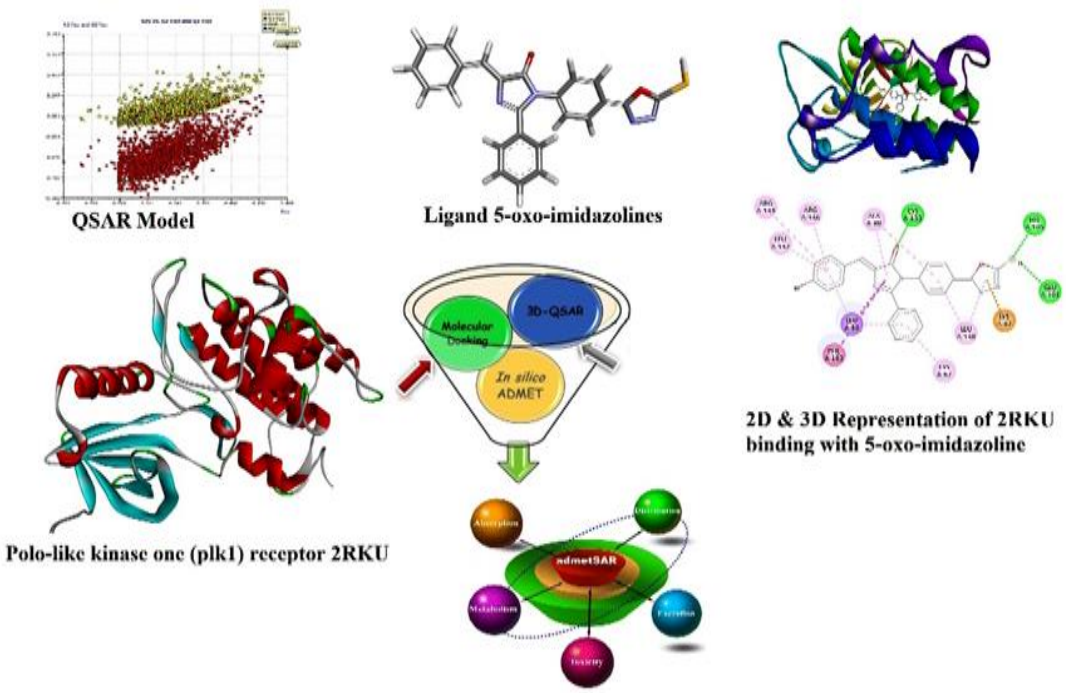

Introduction

Uncontrolled cell multiplication, which affects the surrounding tissue and spreads throughout the body repeatedly, is how cancer is defined. That is a challenging problem [1]. Cancer is the most dreadful disease and a massive cause of human suffering and death, despite substantial advancements in high technology and social growth [2].

Breast cancer now accounts for one in eight cancer diagnoses and 2.3 million new cases in both sexes combined, replacing lung cancer as the most frequently diagnosed cancer worldwide [3]. According to estimates, 685,000 women have been died from breast cancer in 2020, accounting for 16% of all women's cancer deaths. The World Health Organization (WHO) recently launched the Global Breast Cancer Initiative in response to an earlier inadequate public health response to this development [4]. Patients diagnosed with breast cancer tend to share several characteristics. These include older age, failure to nurse for an adequate period, weight increase, early first pregnancy, inactivity, etc. [5]. Because of an extensive investigation into the processes and pathways by which cancer spreads and the discovery of various anti-cancer drugs, a breakthrough in cancer treatment extensive research into the techniques and ways by which cancer spreads and the discovery of different anti-cancer drugs, a breakthrough has been made in cancer treatment [2].

The progesterone receptor (PR) and oestrogen receptor (ER) positive luminal type of breast cancer (ER) is caused by overexpression of the oestrogen receptor (ER). This group includes about 70% of women with breast cancer identified as ER-positive (ER+). The MCF-7 cell line grows due to estrogens' ongoing ER activation [6]. Polo-like kinase 1 (Plk1) is a master regulator of the mitotic controller process and a popular therapeutic target. Its overexpression in the tumor is usually associated with a poor prognosis for the patient, and it is overexpressed in many different types of cancer [7]. In cancer cells, polo-like kinases (Plk1) promote aggressive proliferation and strong induction of cell-circle formation [8].

Due to genetic ambiguity and subsequent encouragement of mammalian cell modification, overexpression of Plk1 permits cells to circumvent hurdles. The most effective receptor for treating breast cancer has been identified as plk1. In human breast cancer cells, the estrogen receptor (ER), mediated by Plk1, controls gene overexpression. In a recent study, researchers observed that a group of 39 different imidazolone derivatives combined with a chalcone moiety suppressed the proliferation of MCF-7 breast cancer cells [9]. In natural products and artificial compounds, imidazole and its derivatives play an important role because imidazole scaffolds act as a bridge between synthetic organic chemistry and medicinal chemistry as they possess a plethora of biological applications like anticancer, antifungal, antiviral, anti-tubercular, anti-diabetic, anticonvulsant, antiulcer, and urease inhibitory. Since the imidazole molecules are extremely electron-rich and may readily bind to various enzymes and receptors, they exhibit a wide range of antiproliferative activity [10]. Angiotensin II receptor antagonistic activity, anticancer activity, antibacterial activity, cardio-activity, and other features have been demonstrated for compounds containing an imidazolone moiety [11].

Chemotherapy remains a prominent and efficient therapeutic approach. However, its efficacy is sometimes hindered by unfavorable toxicities, including weight loss, exhaustion, nausea, and appetite suppression. Consequently, the search for improved pharmacological alternatives with lower toxicity is imperative in order to effectively combat this condition [12]. The utilization of computer-aided drug design methodology has the advantage of time efficiency and greater efficacy in the development of therapeutic candidates. The objective of this study is to investigate the newly developed imidazolone derivatives through the construction of a quantitative structure-activity relationship (QSAR) model. This model was used to predict the anti-proliferative activities of the compounds. Furthermore, molecular docking studies were done using the derivatives and the plk1 receptor to gain insights into their interactions. The ultimate goal is to contribute to the discovery of anti-breast cancer drugs that are both less toxic and more effective in the treatment of breast cancer.

Materials and Methods

Computer applications

The software package for DS Visualizer 2021 consists of Chem Draw version 12.0.2, CHEMOPY descriptors, Conversion molecular formats open babel, molecular optimisation using Avogadro, and Molecular binding affinity using Auto dock version 4.2.1.

QSAR analysis

Dataset

In the works of Abo-Elanwar *et al.* (2019), 39 derivatives of imidazolones linked to chalcone moiety with anti-proliferative effects (IC_{50}) on MCF-7 cancer cell lines were discovered. The anti-proliferative activity's inhibitory concentration (IC_{50}) was calculated, and the logarithm scale (pIC_{50}) was applied. Table 1 presents the pIC_{50} and the tabular version of the IC_{50}, expressed in quantities of micro molar (Mm) units.

$$pIC_{50} = \log10\ (IC_{50} \times 106).$$

Preparation of Molecular Structures and Optimization of 3D Geometry

The molecular structures were made with Chem Draw Professional 16 and converted into the mol2 format with Open Babel v2.4.1.17 (N.M. O'Boyle *et al*., 2011). To make the molecules' shape when hydrogens were added as optimal as possible, Avogadro V1.2.018 was also used. The molecular modeling force field (MMFF94) was developed using molecular mechanics in 1994 and was combined with the steepest descent method. The Avogadro tool and the "scoring function energy" have been used for each molecule to discover the ideal conformer with the lowest global energy. The same conformer was used for the investigation [13, 14].

Molecular identifiers

Table 1: Compounds in the dataset with structure, code, and experimental pIC_{50} value for *polo-like kinase 1* inhibitory activity

S. No.	Compound	IC50	pIC50
1	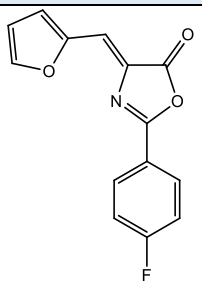	47.84	4.3202
2	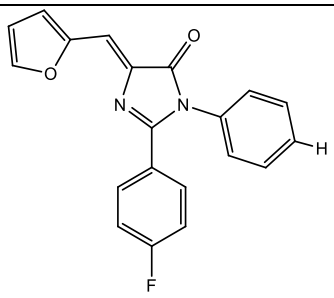	10.36	4.9846
3	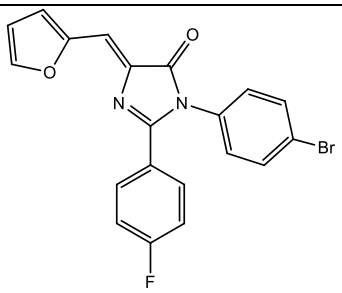	15.81	4.8011
4	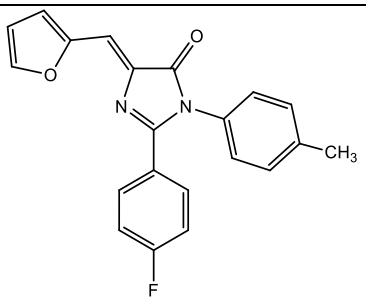	8.67	5.062
5	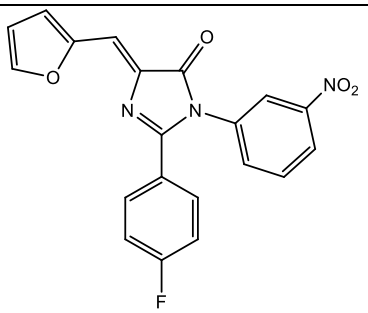	95.37	4.0206
6	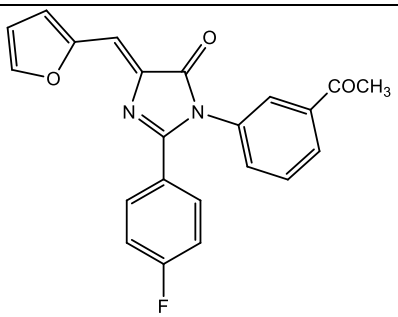	22.87	4.6407

7	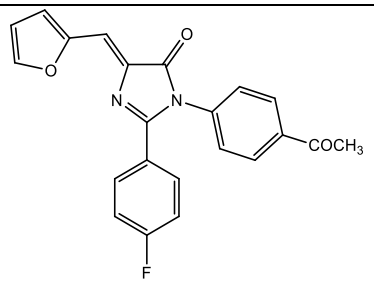	93.62	4.0286
8	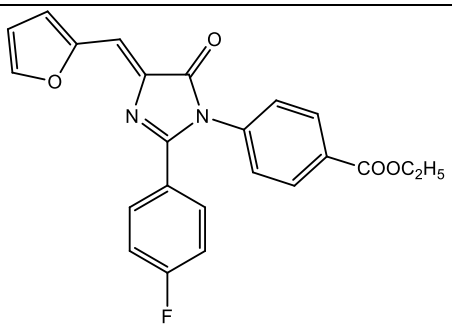	29.84	4.5252
9	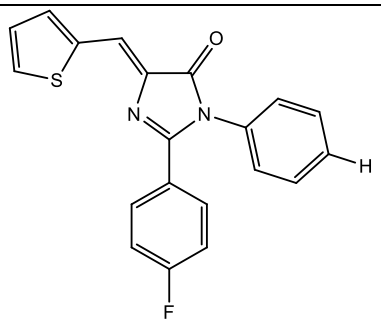	88.25	4.0543
10	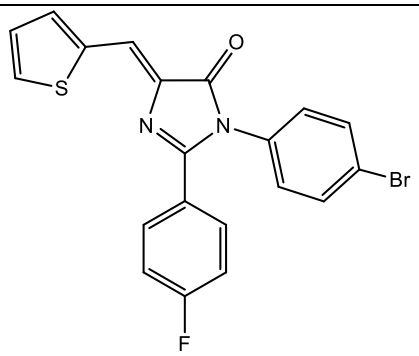	90.50	4.0434
11	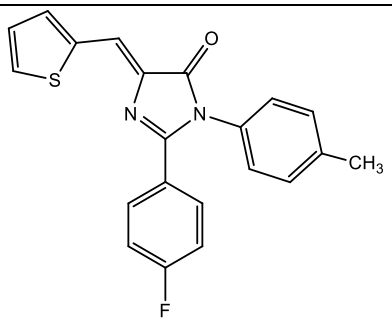	61.06	4.2142
12	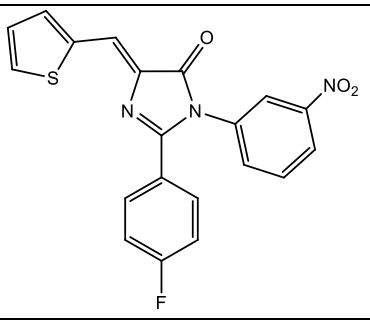	37.80	4.4309

13	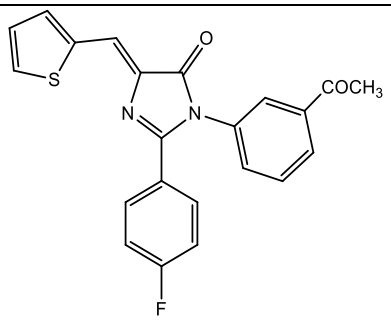	32.62	4.4865
14	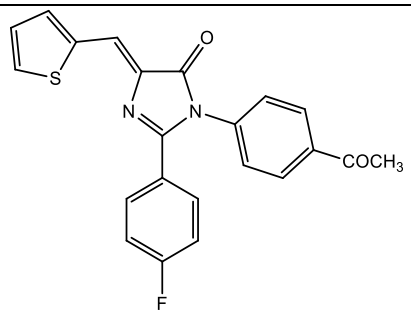	39.57	4.4026
15	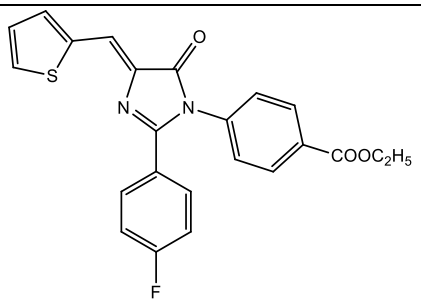	82.62	4.0829
16	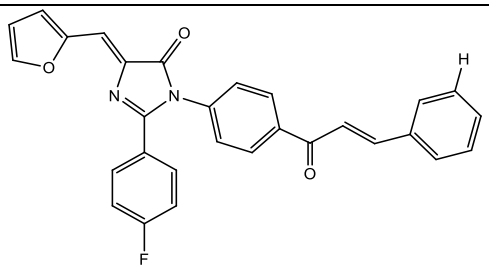	12.59	4.900
17	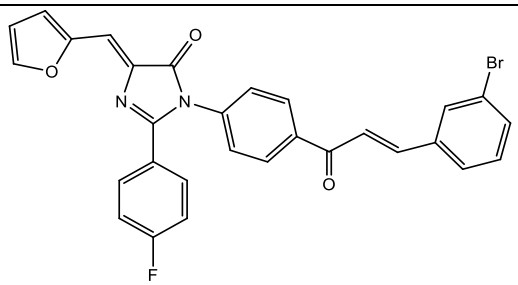	15.37	4.8133
18	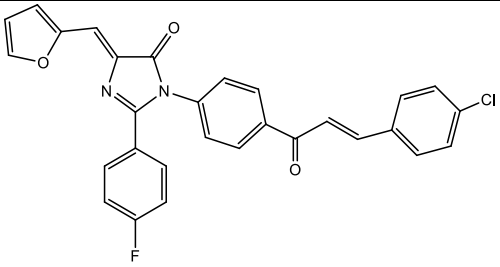	18.85	4.7247

19	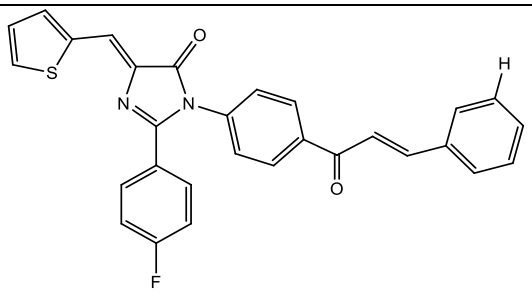	27.50	4.5607
20	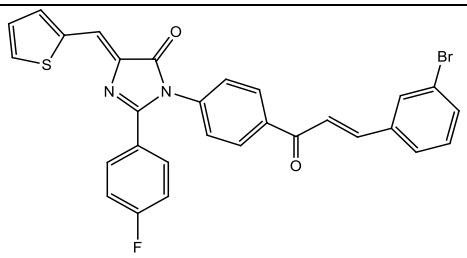	45.42	4.3428
21	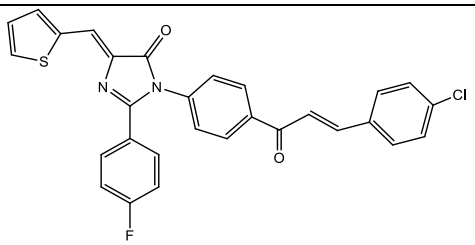	72.65	4.1388
22	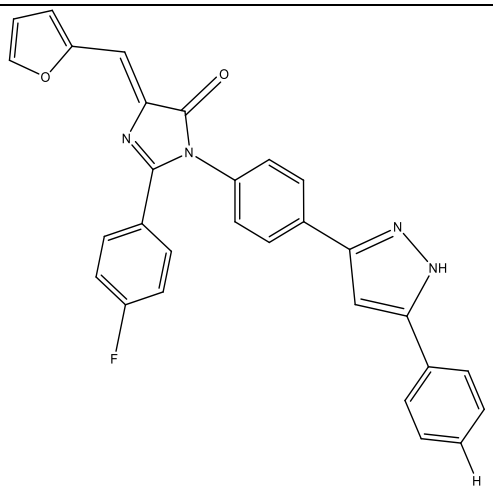	11.72	4.9311
23	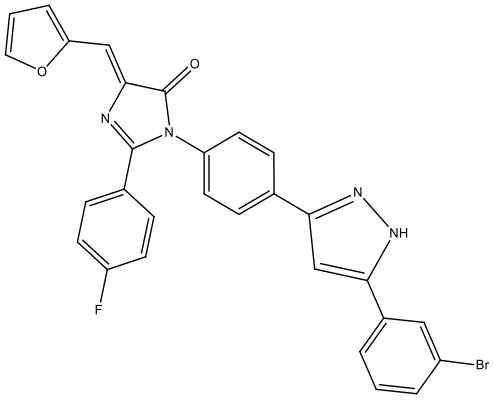	7.58	5.1203

24	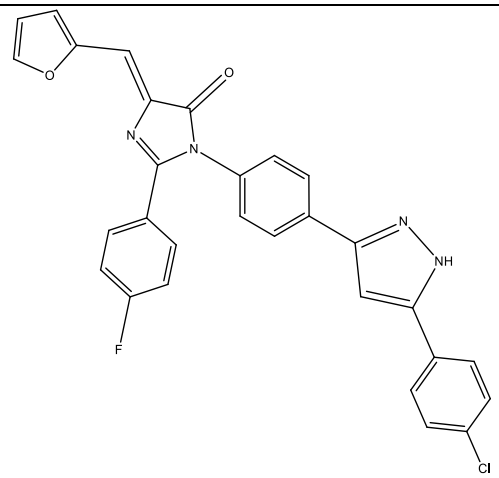	7.83	5.1062
25	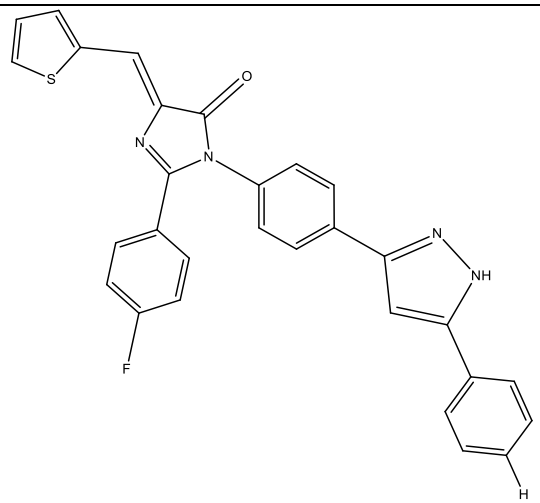	50.10	4.6955
26	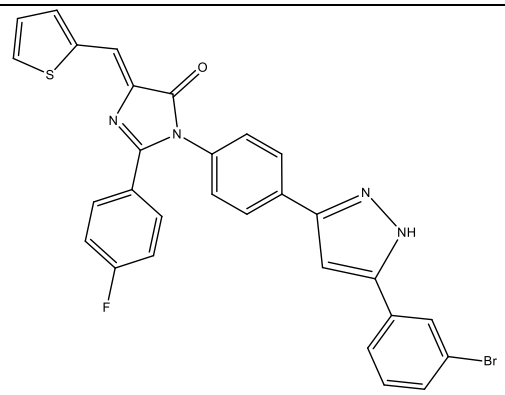	80.41	5.0132
27	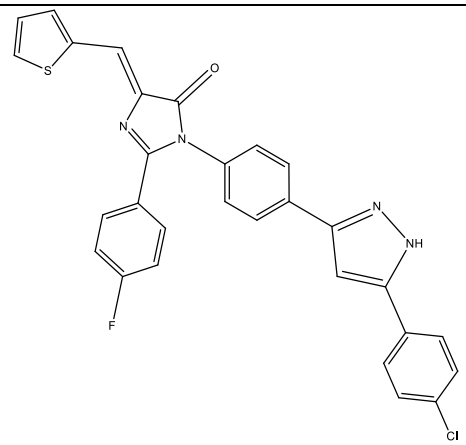	25.81	5.2027

28	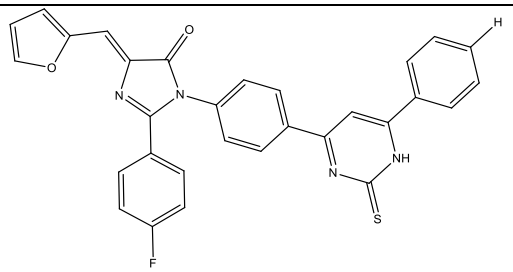	9.48	5.0232
29	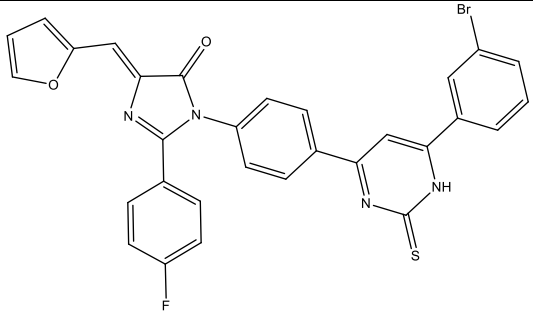	23.61	4.6269
30	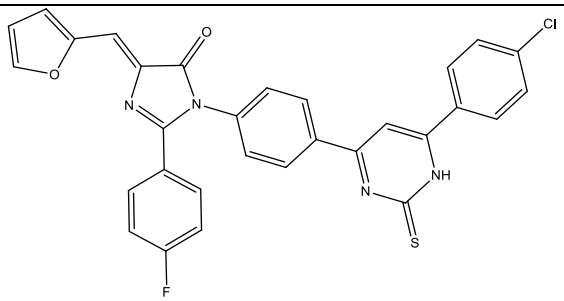	13.66	4.8645
31	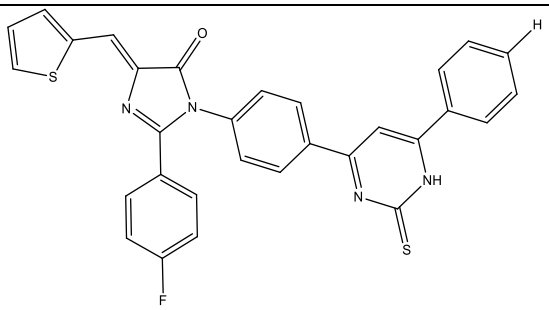	50.10	4.3002
32	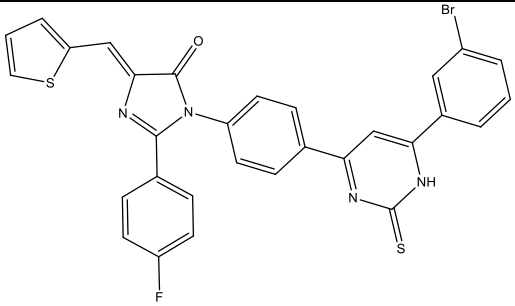	80.41	4.0947
33	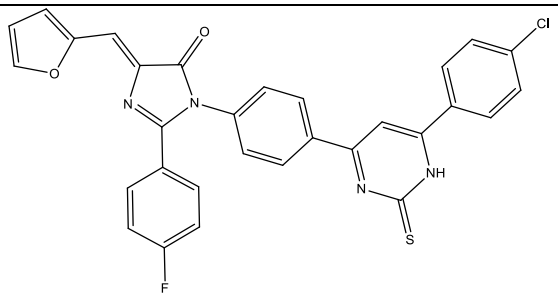	25.81	4.5882

34	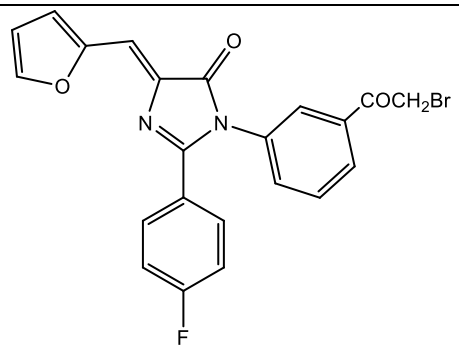	28.13	4.5508
35	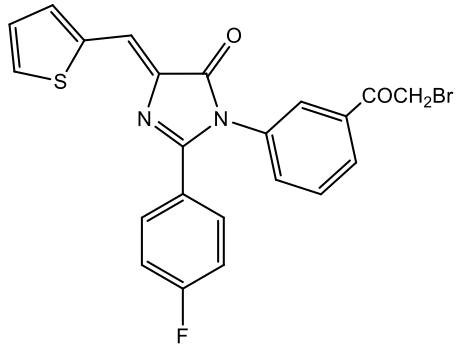	56.92	4.2447
36	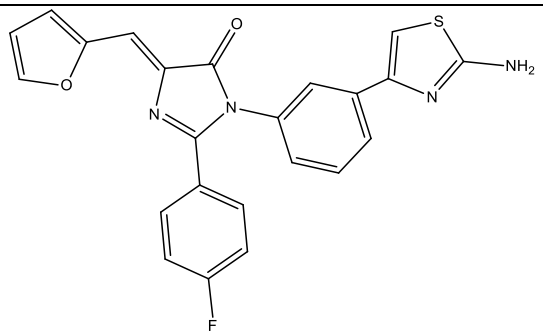	17.63	4.7537
37	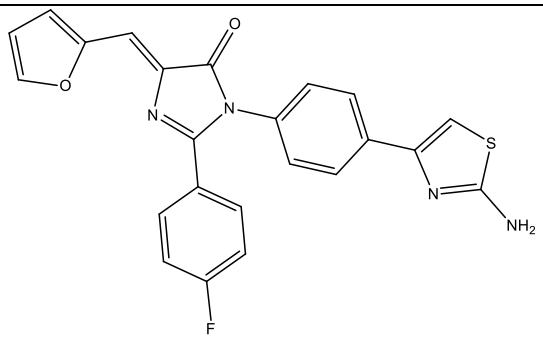	26.49	4.5769
38	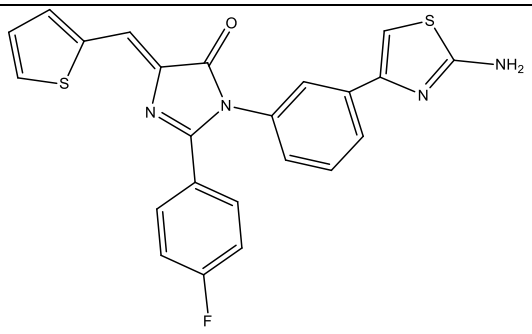	34.81	4.4583

39	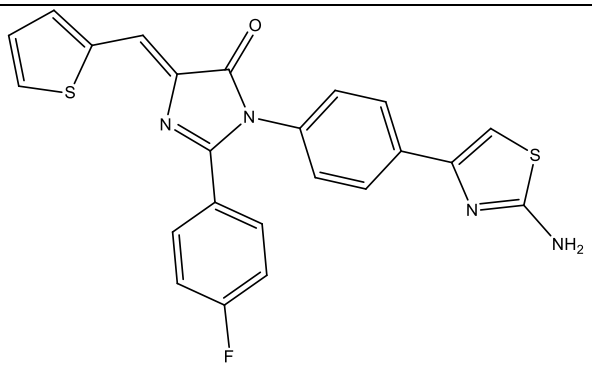	22.03	4.657

The molecular descriptors for the 39 Imidazolone derivatives were optimized and calculated using CHEMOPY Server.

Pre-treatment and division of data set

Using Data Pre-treatment software GUI 1.2, the CHEMOPY Server results were processed to eliminate constant values and undesired descriptors [15]. To create a mathematical equation, the Kennard-Stone approach separated the derivatives into 12 validation sets and 27 calibration sets [16].

QSAR formula

A model was built using the Lack of Fitness Function (LOF) procedure and the QSRINS software. Anti-proliferative activities (pIC_{50}) are the dependent variable, and model parameters are the independent variable. An external data set that has yet to be used during the model-development process should be used to test the validity of the built model [17].

Model validation

Models developed using "QSARINS" were evaluated for applicability and internally and externally validated. Selected models underwent the use of external validation the Q2 F1, Q2 F2, and Q2 F3 techniques, concordance correlation coefficient (CCC), internal validation using the Cross-validation leave-one-out (Q2LOO), Cross-validation leave-many-out (Q2LMO), Root mean squared error (RMSE), and Y-scrambling techniques. During the 5000 Q2LMO runs, 50% of the training set's objects are removed. Y-scrambling aims to eliminate chance association in the initial model by rearranging answer data across 5000 iterations. It is crucial to remember that the R 2 and Q2LOO should be more significant than the more fantastic scrambled ones and that the model's RMSE under prediction should have a lower RMSE. Since it measures the consistency between two variables, the CCC (CCCext) is a tool used to analyze the repeatability of models. Using leverage analysis, the descriptors employed and evaluated establish the theoretical area modeling's applicability domain.

Stepwise regression, fitting with successive additions of descriptors, significantly improved the fit when the model could no longer be improved, and then the descriptors that had the most negligible statistically significant impact on model fit were dropped [18]. The process was repeated until no more descriptors could be deleted without suffering a statistically significant fit loss. Three models were made using these criteria. With the fewest descriptors, the highest (R^2) was found with no descriptor co-linearity and the best prediction model was selected for future development, as provided in Table 2. The models' validity was evaluated using the "leave-one-out" (LOO) cross-validation technique. During the validation step, the model function is trained using data from every molecule but one [19]. The pIC50 for the chemical that was not a part of the study was then predicted using the model's properties. They utilize statistical measures like Q_2 (cross-validated correlation coefficient), R^2 (regression coefficient), SD (standard deviation), and SE (standard error) in the proposed QSAR models [20].

The least necessary values for evaluating the mathematical equation are listed in Table 2. The

table parameters adjusted the derived equations' effectiveness and predictive capability [21].

ADME and drug-likeness predictions

To ascertain their pharmacological similarity, the best-fitting ligands obtained by molecular docking were put through ADME analysis. The ADME forecasts were created using a web application called Swiss ADME. A few characteristics (HIA) were Lipophilicity LogP, molar solubility in water LogS, BBB permeability, skin permeation, and human gastrointestinal absorption. The synthetic accessibility was predicted using a score from 1 to 10, where one indicates that the synthetic route is fairly pretty forward and ten indicates that the substance's structure is complex and that it is challenging to synthesize, along with such as Lipinski's rule of five, which have drug-like qualities. In addition, the bioavailability score was computed. Using the toxicity prediction, the possible toxicity of the inhibitors was estimated [22].

On Chemdraw Ultra 16.0, the recommended compounds' 2D structures were created to analyze their pharmacokinetic characteristics. When each structure was imported, the structural grin was entered into the (http://swissadme.ch/) interface. The ADMET features and criteria were produced by the Swiss ADME drug design study [23].

Molecular docking

The receptor Polo-like kinase 1(PKL1), in combination with BI2536, was used in molecular docking experiments on five drugs with significant pIC50. The ligand (compounds) were also converted to PBD format as indicated in Figure 1 (Receptor and Ligand 3D structures and the receptor was retrieved from Protein Data Bank (Code: 2RKU) and set using Discovery Studio software. To determine the binding affinity of the ligand and receptor, Autodock version 4.2.6 was used [24].

Results and Discussion

QSAR model developed and designed structures

Polo-like kinase (plk1) inhibitor compounds 1-39 were discovered using the pharmacological data of 39 5-oxo-Imidazoline derivatives from the literature (Table 1). As a measure of physiological activity, pIC_{50} ($logIC_{50}$) was employed, and IC50 values represent the concentration of a chemical required to inhibit 30% of the tested in identical experimental conditions. Using principal component regression (PCR) and partial least square regression (PLS), it was determined whether there was a linear relationship between the IC_{50} and the relevant descriptors. The best prediction model, however, was produced by MLR, which included the fewest predictive elements and a high regression coefficient (R^2) of the most crucial variables.

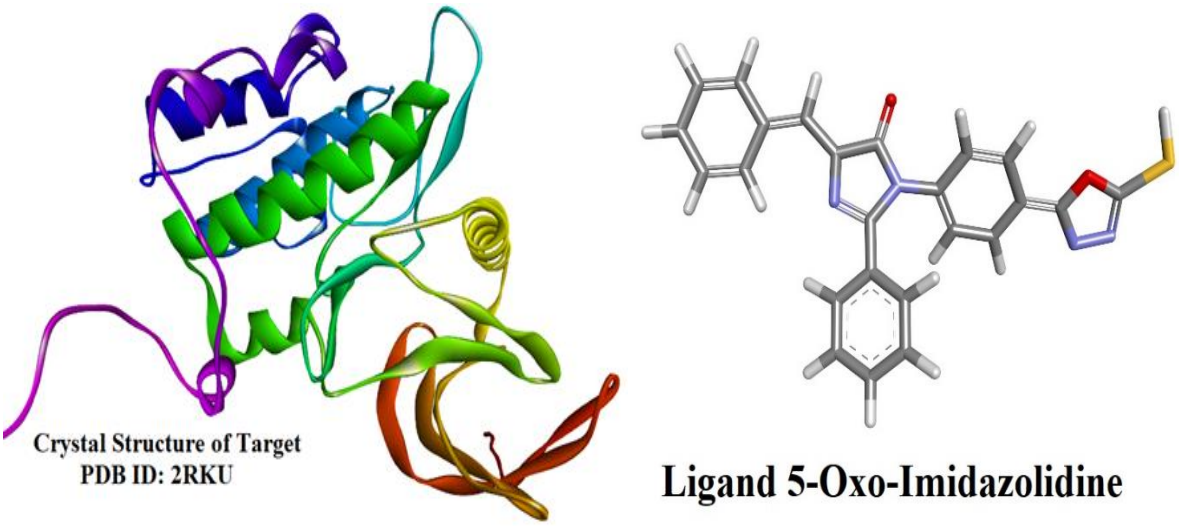

Figure 1: 3D Representation of prepared ligand-receptor

Model 01 was developed using MLR, and the descriptors had a standard error (SE) of 0.374 and accounted for 57% of the variation in biological activity.

Model 1

pIC50 = -3.4611 +2.6571*(Hato) +3.1781*(bcutp14) +1.5499*(MORSEC1)+-0.0429* (RDFU14)

n_{tr} = 39 n_{pred} = R^2=0.7429 R^2adj= 0.7061 R^2-R^2adj = 0.0367 LOF = 0.0541K_{xx} = 0.3885 $Delta_K$ = 0.0714 $RMSE_{tr}$ = 0.1762 MAE_{tr} = 0.1433RSS_{tr} = 1.0241 CCC_{tr} = 0.8525 s = 0.1912 F =20.2223Q_{2loo} = 0.3558 R^2-Q_{2loo} = 0.1101 $RMSE_{cv}$ = 0.2105 MAE_{cv} = 0.1702$PRESS_{cv}$ = 1.4625 CCC_{cv} = 0.7954 Q_{2LMO} = 0.6076 R_{2Yscr} = 0.1289 Q_{2Yscr} = -0.2219 $RMSE_{AVYscr}$ = 0.3239$RMSE_{ext}$ =0.3697 MAE_{ext} = 0.3167 $PRESS_{ext}$ = 0.8199 R^2_{ext} = 0.6726 $Q_{2\text{-}F1}$ = -0.2977 $Q_{2\text{-}F2}$ = -0.3627 $Q_{2\text{-}F3}$ = -0.1322 CCC_{ext} = 0.6877$r^2_{m\ aver}$ = 0.2370 $r^2_{m\ delta}$ = 0.4976.

Model 1 fits well and yields positive internal validation findings. With no outliers in William's figure, the external validation parameter values have somewhat decreased from the prior model. The descriptor correlation matrix for Model 1 is presented in Table 2. Figure 2 shows a scatter plot of the inhibitory actions of 5-oxo-imidazolines on polo-like kinase1, with expected values roughly matching the actual values. The final model's Kxy (inter-correlation among descriptors and response) versus Q2 LMO is depicted in Figure 3, and it demonstrates that the model is robust and stable because the "Leave many out" parameter values were near the model parameters. The structure-response relationship is broken, as the correlation coefficients of the final model are much higher than those obtained after endpoint scrambling Figure 4, which shows a Y-scramble plot of Kxy versus R2Yscr and Q2Yscr. In Figure 5, the forecast and the model's applicability range were illustrated using William's plot of standardized residuals vs. leverage levels. According to William's figure, all the compounds have leverage values lower than the warning h* of 0.462. They are in the model's application domain Figure 6. The importance of Q2F1, Q2F2, and Q2F3 are almost identical and of higher value as the CCC (concordance correlation coefficient) parameter values are raised. These results suggest that the best model was not found by accident and that the 5-oxo-imidazolines structure and polo-like kinase1 inhibitory activity are related.

In QSAR/QSPR studies, the 3D-MoRSE method was frequently applied, which creates representations of three-dimensional molecular structures using electron diffraction descriptors. Interatomic distances, scattering parameters (0–31 integer values), weighting by atomic properties like atomic charges (RDFC24), total surface area (PSA), MOE descriptors (EstateVSA5), and nuclear polarizability (MoRSEP3), as well as Moran autocorrelation, log 5 weighted by atomic polarizabilities (MATSP5), are some of the sources from which these data are derived. Compounds can be made more sensitive to the presence of particular molecular fragments using weighted descriptors.

In other words, the partial atomic charge can be used to calculate the distance between atoms having a high or low electron density. As the scattering parameters rise, the 3D-MoRSEC1 descriptors weighted with hydrogen-lighter schemes ought to exhibit less variation. Atomic mass, Van der Waals volume, and polarizability weightings have the least significant relative change in comparison, according to the literature. Distinct interatomic lengths may have distinct impacts, as shown by the dynamics of the cumulative sum of 3D-MoRSEC1 terms categorized by interatomic distance.

Table 2: The best model's correlation matrix

Descriptors	Hato	bcutp14	MoRSEC1	RDFU14
Hato	1.0000			
bcutp14	0.4091	1.0000		
MoRSEC1	0.0967	-0.1763	1.0000	
RDFU14	0.3448	0.8331	-0.0858	1.0000

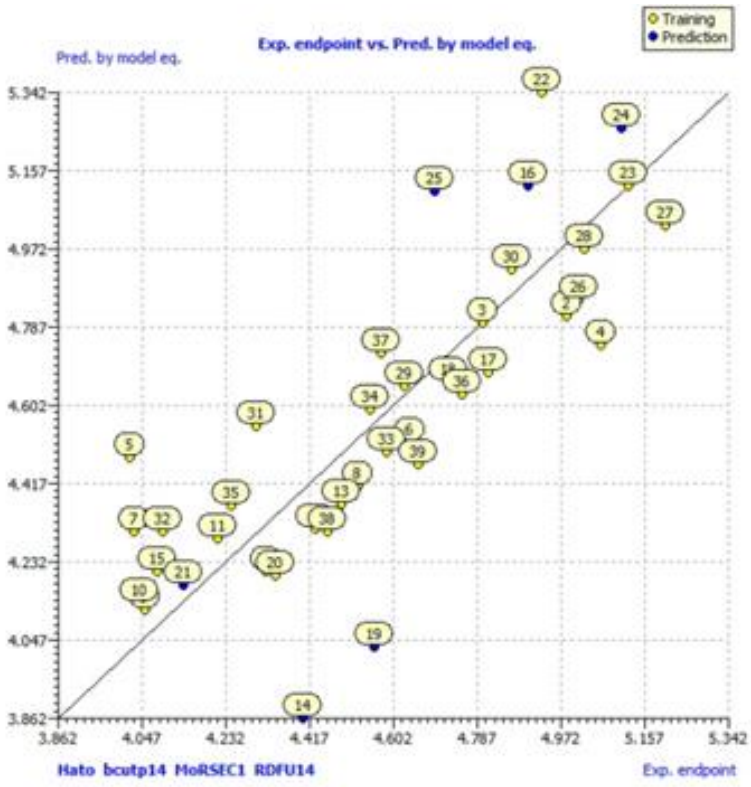

Figure 2: Scatter diagram of dataset compounds based on testing results of the best model equation

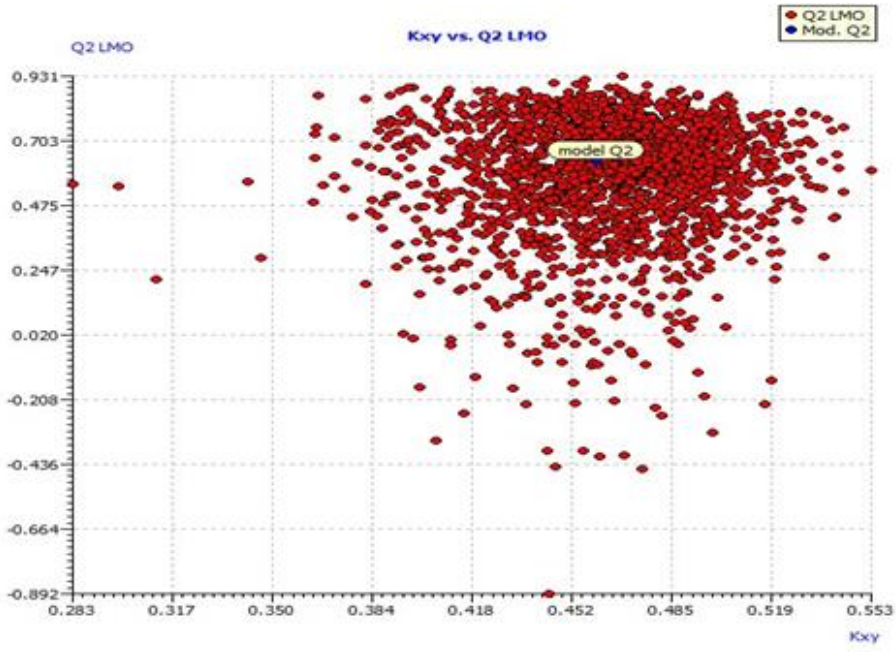

Figure 3: Visualization of dataset compounds using LMO scatter plots based on experimental values from the best model equation

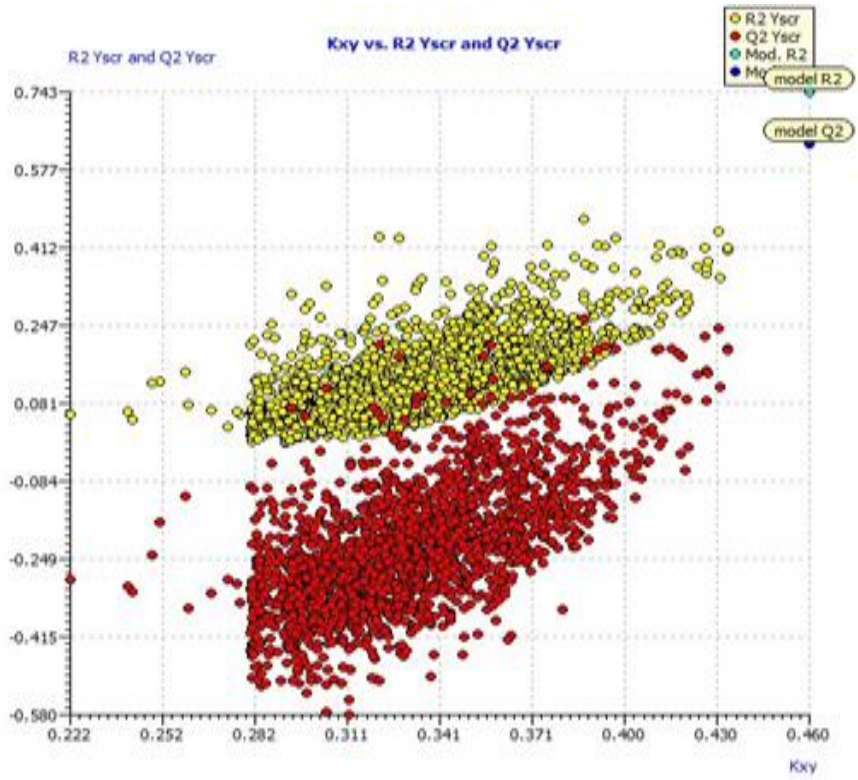

Figure 4: Layout with a Y-scramble

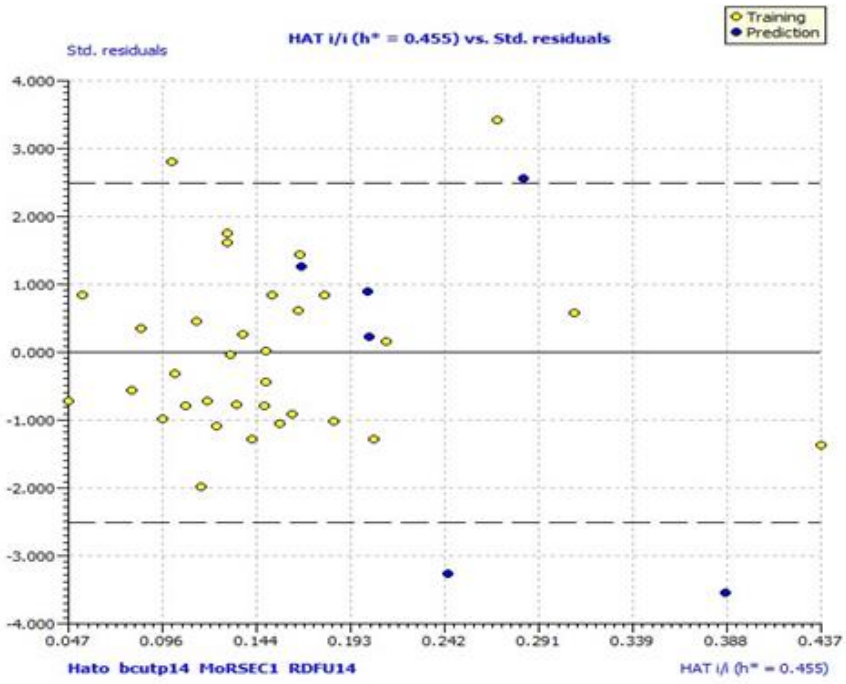

Figure 5: The best model plot by William (h*, 0.455) warning value

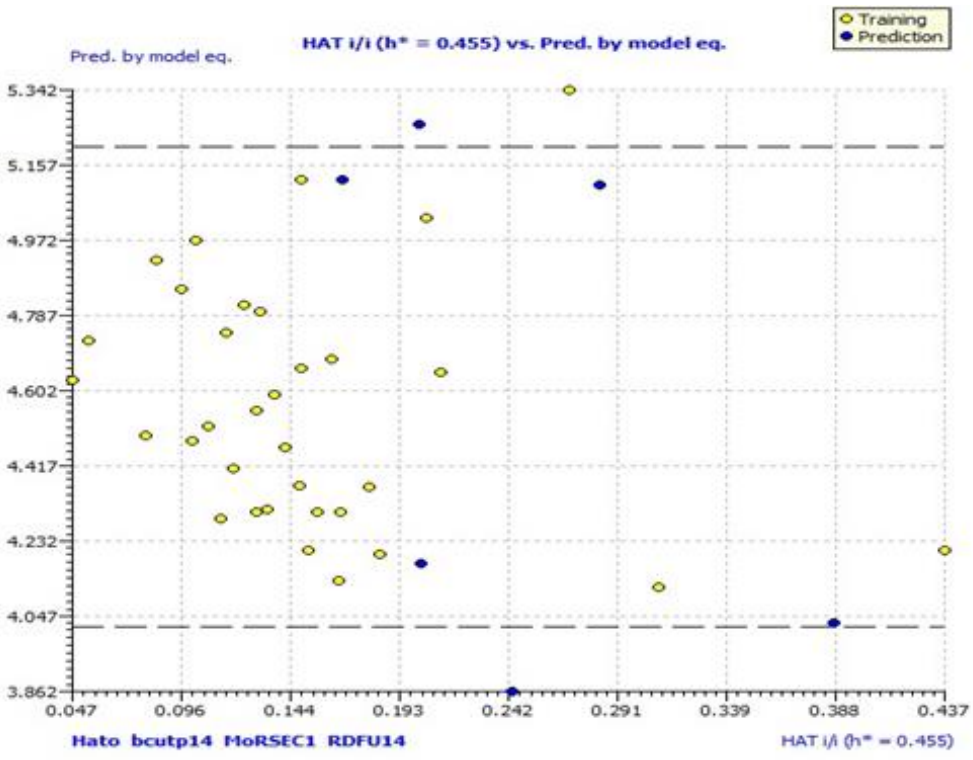

Figure 6: Applicability domain plot of William's best model

Understanding the optimal interatomic distance in active compounds and comparing it to non-active compounds may help interpret 3D-MoRSEC1 descriptors by identifying the appropriate range of MoRSEC1 values required for the best activity, and thus aid in the interpretation of 3D-MoRSEC1 descriptors [25]. The connection between each descriptor in Model 1 and the activity is positive. The final model was used to calculate the pIC_{50} values for each drug, which are displayed in Table 3.

SAR of original data

Electron-withdrawing groups are substituted on the R1 position of the phenyl ring to improve the inhibitory activity of polo-like kinase 1, and based on the SAR analysis conducted on the original dataset utilizing molecular descriptors, it was seen that the incorporation of 5-mercapto-1,3,4 oxadiazole rings fused with a 5-oxo-imidazoline ring system resulted in a notable decrease in movement. In contrast, substituting a bulky and lipophilic group at the R1 position increased the activity. Hydrophilic substituents like methoxy and hydroxyl at the R1 position of the 5-oxo-imidazoline ring have been shown to improve *polo-like kinase 1* activity (Scheme 1). The 5-oxo-imidazoline R2 position was substituted with various heterocyclic rings showed good activity Table 4. The analysis of the pki value using the model equation using molecular descriptors optimized compounds from the Chemopy server is shown in Table 5. Furthermore, molecular docking tests were carried out using combinations with greater pki values.

ADME Properties

It was discovered that ADMET disclosed a number of the physical and chemical characteristics of these novel molecules. These consist of additional factors, qualities, and the five principles of molecular synthesis (iLOGP). Number of heavy aromatic atoms (nAH), molecular weight (MW), rotatable bonds (RB), number of hydrogen bond donors and acceptors (HBD), octanol/water partition coefficient (iLOGP), molecular refractivity (MR), topological polar surface area (TPSA), and iLOGP. As demonstrated in Table 6, none of the synthesized compounds violates Lipinski's rule of five or the notion of drug-like properties more than once.

Table 3: The Best model equation predicted the PIC_{50} values of the original dataset

Name	Pki	Hato	bcutp14	MoRSEC1	RDFU14	PIC_{50}	Residual
1	4.3202	2	0.966	-0.24	7.985	4.2096121	0.1105879
2	4.9846	2.055	1.3	-0.338	18.495	4.8144688	0.1701312
3	4.8011	2	1.3	-0.341	15.382	4.7972263	0.0038737
4	5.062	2	1.3	-0.32	17.317	4.7467627	0.3152373
5	4.0206	1.953	1.327	-0.476	16.968	4.4808754	-0.4602754
6	4.6407	1.953	1.351	-0.453	18.799	4.5142476	0.1264524
7	4.0286	1.953	1.318	-0.464	20.877	4.3031752	-0.2745752
8	4.5252	1.957	1.417	-0.527	23.629	4.412731	0.112469
9	4.0543	2.055	1.125	-0.556	13.891	4.1179347	-0.0636347
10	4.0434	2	1.124	-0.559	9.913	4.1346226	-0.0912226
11	4.2142	2	1.178	-0.545	10.818	4.2891141	-0.0749141
12	4.4309	1.953	1.327	-0.667	13.991	4.3125578	0.1183422
13	4.4865	1.953	1.351	-0.67	14.345	4.3689959	0.1175041
14	4.4026	1.953	1.318	-0.834	17.806	3.8614581	0.5411419
15	4.0829	1.957	1.411	-0.765	19.338	4.2088701	-0.1259701
16	4.9	2.039	1.511	-0.445	22.117	5.1213112	-0.2213112
17	4.8133	2	1.511	-0.449	29.835	4.6803825	0.1329175
18	4.7247	2	1.511	-0.471	29.533	4.6592405	0.0654595
19	4.5607	2.039	1.444	-0.84	28.31	4.0304883	0.5302117
20	4.3428	2	1.444	-0.698	27.054	4.2008296	0.1419704
21	4.1388	2	1.444	-0.703	27.399	4.1782796	-0.0394796
22	4.9311	2.118	1.511	-0.389	23.902	5.34144	-0.41034
23	5.1203	2.075	1.511	-0.38	26.646	5.1234162	-0.0031162
24	5.1062	2.075	1.511	-0.382	23.409	5.2591837	-0.1529837
25	4.6955	2.118	1.487	-0.604	19.744	5.1103153	-0.4148153
26	5.0132	2.075	1.481	-0.595	22.953	4.8532744	0.1599256
27	5.2027	2.075	1.48	-0.596	18.734	5.0295415	0.1731585
28	5.0232	2.073	1.511	-0.479	26.456	4.9728129	0.0503871
29	4.6269	2.035	1.511	-0.464	32.179	4.6495749	-0.0226749
30	4.8645	2.035	1.511	-0.477	25.324	4.9235057	-0.0590057
31	4.3002	2.073	1.447	-0.717	22.893	4.553391	-0.253191
32	4.0947	2.035	1.447	-0.7	26.924	4.3058396	-0.2111396
33	4.5882	2.035	1.447	-0.711	22.146	4.4937669	0.0944331
34	4.5508	1.955	1.326	-0.464	14.865	4.591829	-0.041029
35	4.2447	1.955	1.326	-0.682	12.24	4.3665633	-0.1218633
36	4.7537	2.044	1.406	-0.594	20.748	4.6286912	0.1250088
37	4.5769	2.044	1.408	-0.566	19.631	4.7263639	-0.1494639
38	4.4583	2.044	1.404	-0.799	20.741	4.3049058	0.1533942
39	4.657	2.044	1.406	-0.776	18.044	4.462611	0.194389

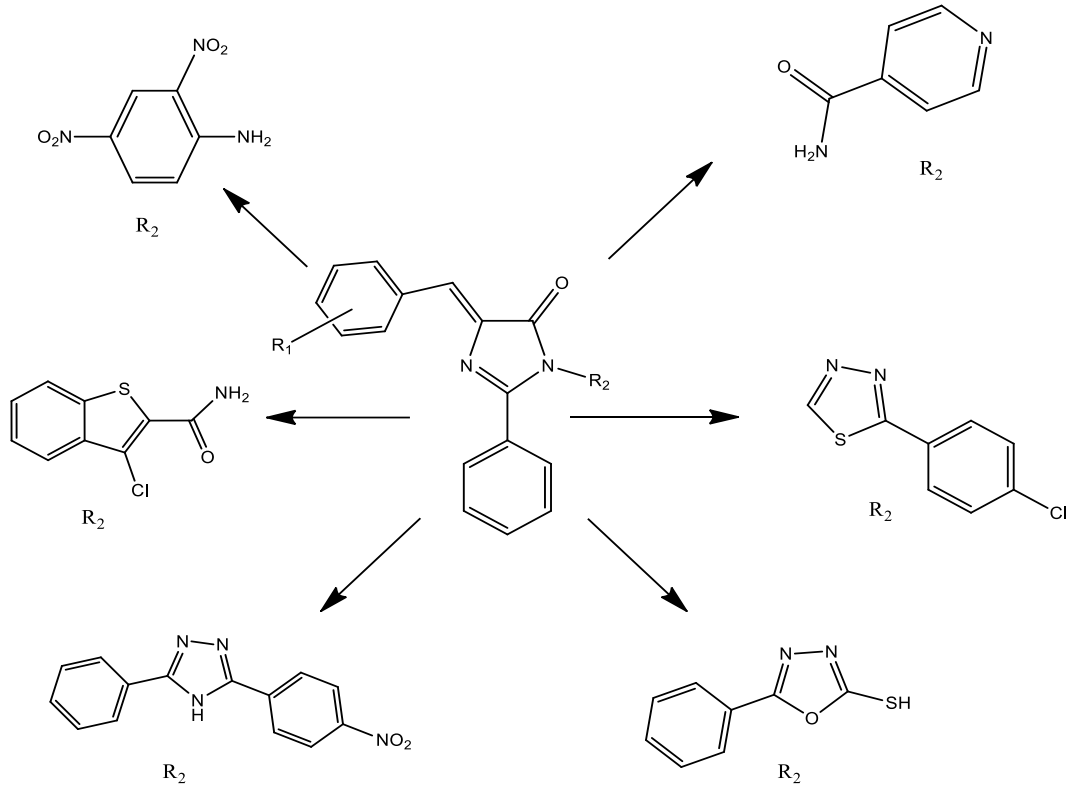

Scheme 1: SAR of designed novel 5-Oxo

Table 4: Designed novel 5-oxo-Imidazolinone compounds

	1a-6a	1b-6b	1c-6c	1d-6d	1e-6e	1f-6f
R_1	4-NO_2	4-OH	4-F	4-Cl	4-Br	4-OCH_3
	1a-f	2a-f	3a-f	4a-f	5a-f	6a-f
R_2	3-(4-nitrophenyl)-5-phenyl-1,2,4-triazole	5-phenyl-1,3,4-oxadiazole-2-thiol	2-(4-chlorophenyl)-1,3,4-thiadiazole	isonicotinamide	2,4-dinitroaniline	3-chlorobenzothiophene-2-carboxamide

Table 5: 2D structure, descriptor values, and predicted activity pIC_{50} for newly developed compounds

Name	Hato	bcutp14	MoRSEC1	RDFU14	PIC_{50}
1a	2.078	1.521	-0.94	23.214	4.442457
1b	2.184	1.516	-0.691	21.916	5.149829
1c	2.234	1.514	-0.655	22.893	5.290211
1d	2.764	1.511	-0.616	22.069	6.784735
1e	2.418	1.51	-0.602	21.915	5.890506
1f	2.198	1.519	-0.653	22.2	5.243275
2a	2.586	1.391	-0.612	22.433	5.920983
2b	2.243	1.39	-0.355	23.198	5.371926
2c	2.365	1.39	-0.321	22.927	5.760414
2d	2.843	1.39	-0.28	22.956	7.09281
2e	2.862	1.39	-0.267	22.698	7.174512
2f	2.698	1.391	-0.316	27.757	6.448949
3a	2.294	1.301	-0.67	15.972	5.046364
3b	2.458	1.282	-0.413	14.274	5.892913
3c	2.458	1.282	-0.374	15.779	5.888794

3d	2.758	1.282	-0.337	16.3	6.72092
3e	2.745	1.282	-0.322	17.407	6.662136
3f	2.568	1.339	-0.38	16.239	6.333194
4a	1.958	1.301	-0.709	17.646	4.021317
4b	2	1.192	-0.471	18.144	4.134015
4c	2	1.191	-0.44	19.217	4.132852
4d	2	1.191	-0.395	20.022	4.168063
4e	2	1.191	-0.367	16.966	4.342562
4f	2	1.339	-0.417	24.407	4.416207
5a	1.858	1.455	-1.196	24.312	3.204262
5b	1.886	1.453	-0.956	23.343	3.685851
5c	1.886	1.452	-0.917	25.594	3.646551
5d	1.886	1.451	-0.879	25.157	3.721016
5e	1.886	1.451	-0.866	25.291	3.735416
5f	1.889	1.454	-0.917	22.956	3.774049
6a	1.963	1.366	-0.898	17.773	3.9428
6b	2	1.366	-0.62	17.122	4.499913
6c	2	1.366	-0.585	16.743	4.570418
6d	2	1.366	-0.545	16.614	4.637949
6e	2	1.366	-0.528	16.723	4.659621
6f	2	1.366	-0.576	20.307	4.431472

Table 6: ADME properties of designed the compounds

Compound	M.W	iLOGP	H.B.D	H.B.A	TPSA	R.B	n.AH	M.R
1a	558.5	3.88	0	9	163.23	7	29	163.96
1b	529.5	3.77	1	8	137.64	6	29	157.16
1c	531.49	4.17	0	8	117.41	6	29	155.09
1d	547.95	4.38	0	7	117.41	6	29	160.15
1e	592.4	4.45	0	7	117.41	6	29	162.84
1f	543.53	4.37	0	8	126.64	7	29	161.63
2a	469.47	3.67	0	7	156.21	5	23	136.95
2b	440.47	3.61	1	6	130.62	4	23	130.15
2c	442.46	4.03	0	6	110.39	4	23	128.09
2d	458.92	4.23	0	5	110.39	4	23	133.14
2e	503.37	4.31	0	5	110.39	4	23	135.83
2f	454.5	4.24	0	6	119.62	5	23	134.62
3a	487.92	3.82	0	6	132.51	5	23	140.32
3b	458.92	3.41	1	5	106.92	4	23	133.52
3c	460.91	3.9	0	5	86.69	4	23	131.46
3d	477.37	4.07	0	4	86.69	4	23	136.51
3e	521.82	4.39	0	4	86.69	4	23	139.2
3f	472.95	4.07	0	5	95.92	5	23	137.99
4a	413.39	2.24	1	6	120.48	6	18	121.68
4b	384.39	2.18	2	5	94.89	5	18	114.88
4c	386.38	2.68	1	5	74.66	5	18	112.81
4d	402.83	2.86	1	4	74.66	5	18	117.86
4e	447.28	2.81	1	4	74.66	5	18	120.55
4f	398.41	2.78	1	5	83.89	6	18	119.35
5a	474.38	2.28	1	8	182.16	7	18	137.83

5b	445.38	1.76	2	7	156.57	6	18	131.04
5c	447.38	2.66	1	7	136.34	6	18	128.97
5d	463.83	2.61	1	6	136.34	6	18	134.02
5e	508.28	2.48	1	6	136.34	6	18	136.71
5f	459.41	2.65	1	7	145.57	7	18	135.5
6a	502.93	3.66	1	5	135.83	6	21	144.27
6b	473.93	3.35	2	4	110.24	5	21	137.48
6c	475.92	3.83	1	4	90.01	5	21	135.41
6d	492.38	4.11	1	3	90.01	5	21	140.46
6e	536.83	4.12	1	3	90.01	5	21	143.15
6f	487.96	3.95	1	4	99.24	6	21	141.94

Discussion of the QSAR Model Generated with Imidazolone Derivatives

The results of the QSAR analysis demonstrated that the lowest possible estimates for the variables in the equation, as indicated in Table 2, were in agreement with the model's internal consistency and its external applicability. Using the validation compounds' model parameters shown in Tables 3 and 4, model 1 external validation was accomplished. The validity compounds dependability, and the calculated pIC_{50} of the calibration compounds were used to gauge the equation's efficacy.

Table 5 displays the biological, calculated, and residual values of compounds that are novel 5-oxo-imidazoline derivatives. The biological and calculated activities differ resulting in low residual values, demonstrating the high predicted Model 1. It is confirmed to be highly effective, robust, and significantly predictive by both internal and external validation. The definition of the model 1 parameter is shown in Table 6. The average effect of the model parameters reveals that (Hato, bcutp14, MoRSEC1, and RDFU14) carry positive coefficients, indicating bioactivities of the compounds would improve with a rise in those variables, while (RDFU14), which brings a negative coefficient, demonstrates that when the descriptor is lowered, the amount of experimentation performed by compounds derived from our novel 5-oxo-imidazoline derivatives. The statistical analysis indicates that the model parameters are not collinear, resulting in a robust equation, as shown in Table 6.

The pIC_{50} correlates well with the observed biological activity, as seen in Table 3, according to the graph of calculated activities (pIC_{50}) against biological activities (IC_{50}) displayed in Figure 1. Figure 2 shows that the values of both the calibration and validation compounds are distributed evenly across both sides of the graph, indicating that there are no systematic inaccuracies between the standardized residual versus bio-activities (Experimental activity). Figure 3 displays William's graph (standardized residuals vs. leverages), which reveals that all of the molecules were located inside the calculated warning leverage area of ($h^* = 0.56$).

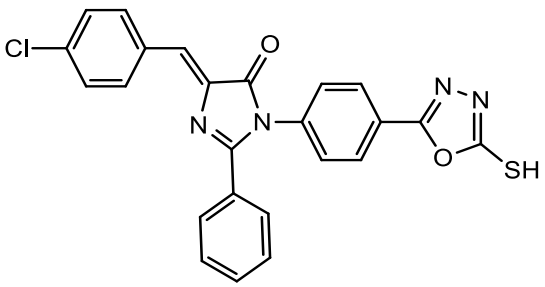

Compound 2d

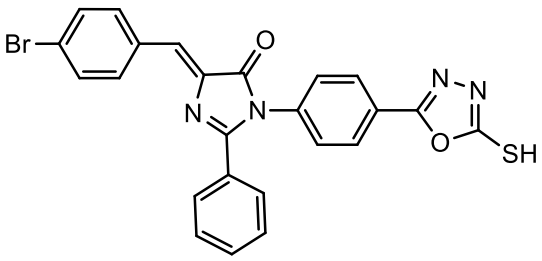

Compound 2e

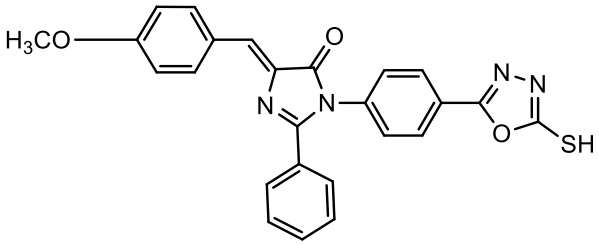

Compound 2f

Scheme 2: Structures of best compounds on molecular docking studies

Table 7: Molecular docking interaction in some complexes

Complex	Binding affinity (kcal/mol)	Amino acid	Bond type	Interaction	Distance (A^0)
2e	-11.33	HIS105	Hydrogen Bond	Conventional Hydrogen Bond	2.11959
		CYS133	Hydrogen Bond	Conventional Hydrogen Bond	2.37364
		GLU101	Hydrogen Bond	Conventional Hydrogen Bond	1.86154
		LYS82	Hydrogen Bond	Pi-Donor Hydrogen Bond	2.50461
		LYS82	Electrostatic	Pi-Cation	2.50461
		LEU59	Hydrophobic	Pi-Sigma	3.62131
		HIS105	Other	Pi-Sulfur	3.97023
		PHE183	Hydrophobic	Pi-Pi Stacked	5.4754
		ALA80	Hydrophobic	Pi-Alkyl	4.31134
		LEU130	Hydrophobic	Pi-Alkyl	5.46377
		LYS82	Hydrophobic	Pi-Alkyl	5.20906
		LEU130	Hydrophobic	Pi-Alkyl	4.95068
		LEU59	Hydrophobic	Pi-Alkyl	4.67461
		CYS67	Hydrophobic	Pi-Alkyl	4.15829
		LEU59	Hydrophobic	Pi-Alkyl	5.12878
		LEU132	Hydrophobic	Pi-Alkyl	5.02082
		ARG134	Hydrophobic	Pi-Alkyl	4.86342
		ARG136	Hydrophobic	Pi-Alkyl	4.66812
2f	-11.12	CYS133	Hydrogen Bond	Conventional Hydrogen Bond	2.2082
		ASP194	Hydrogen Bond	Conventional Hydrogen Bond	1.75903
		ARG134	Hydrogen Bond	Conventional Hydrogen Bond	1.93115
		ARG57	Electrostatic	Pi-Cation	4.08366
		LEU59	Hydrophobic	Pi-Sigma	3.59311
		LEU130	Hydrophobic	Pi-Sigma	3.31388
		PHE183	Hydrophobic	Pi-Pi Stacked	4.42302
		LEU130	Hydrophobic	Alkyl	4.07701
		HIS105	Hydrophobic	Pi-Alkyl	4.25927
		ALA80	Hydrophobic	Pi-Alkyl	4.27594
		LEU59	Hydrophobic	Pi-Alkyl	4.25373
		ARG136	Hydrophobic	Pi-Alkyl	4.21061
		ARG136	Hydrophobic	Pi-Alkyl	4.48208
		LEU59	Hydrophobic	Pi-Alkyl	5.13677
		ALA80	Hydrophobic	Pi-Alkyl	5.1518
		VAL114	Hydrophobic	Pi-Alkyl	4.72797
2d	-10.95	LYS82	Hydrogen Bond	Conventional Hydrogen Bond	2.13311

		HIS105	Hydrogen Bond	Conventional Hydrogen Bond	2.22792
		CYS133	Hydrogen Bond	Conventional Hydrogen Bond	2.4672
		GLU101	Hydrogen Bond	Conventional Hydrogen Bond	1.807
		LYS82	Hydrogen Bond	Pi-Donor Hydrogen Bond	2.53939
		LYS82	Electrostatic	Pi-Cation	2.53939
		LEU59	Hydrophobic	Pi-Sigma	3.51737
		HIS105	Other	Pi-Sulfur	4.06051
		PHE183	Hydrophobic	Pi-Pi Stacked	5.60098
		ALA80	Hydrophobic	Pi-Alkyl	4.41362
		LEU59	Hydrophobic	Pi-Alkyl	4.83488
		CYS67	Hydrophobic	Pi-Alkyl	4.35517
		ALA80	Hydrophobic	Pi-Alkyl	4.95273
		LYS82	Hydrophobic	Pi-Alkyl	5.2027
		LEU130	Hydrophobic	Pi-Alkyl	4.97623
		LEU59	Hydrophobic	Pi-Alkyl	5.11885
		LEU132	Hydrophobic	Pi-Alkyl	5.19167
		ARG134	Hydrophobic	Pi-Alkyl	4.98537
		ARG136	Hydrophobic	Pi-Alkyl	4.5843

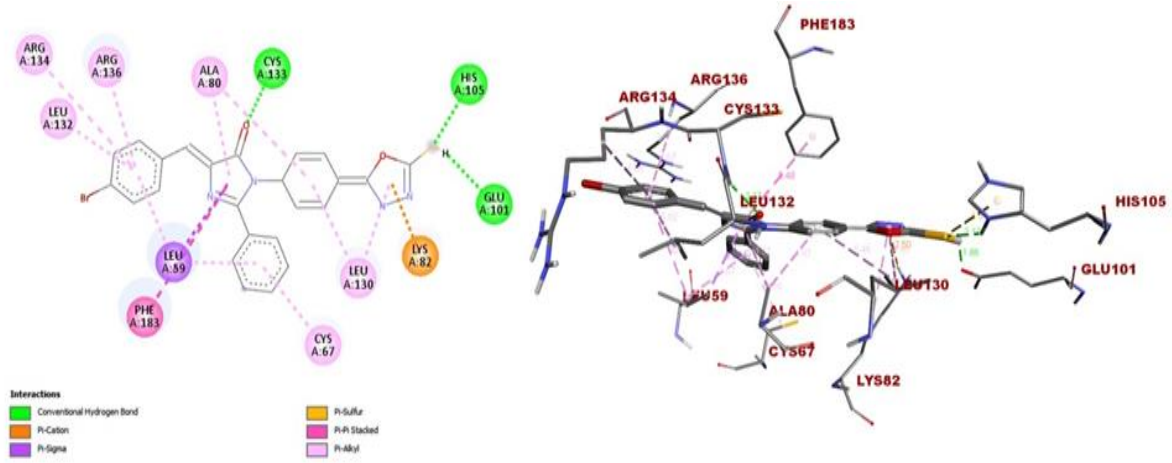

Figure 7: 2D and 3D representation of complex 2e

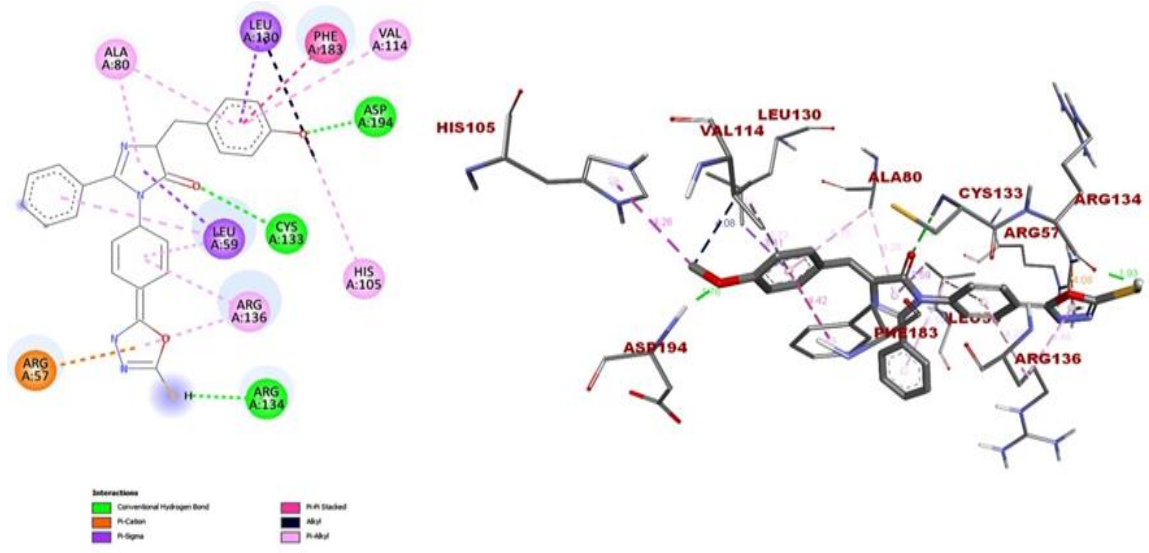

Figure 8: 2D and 3D representation of complex 2f

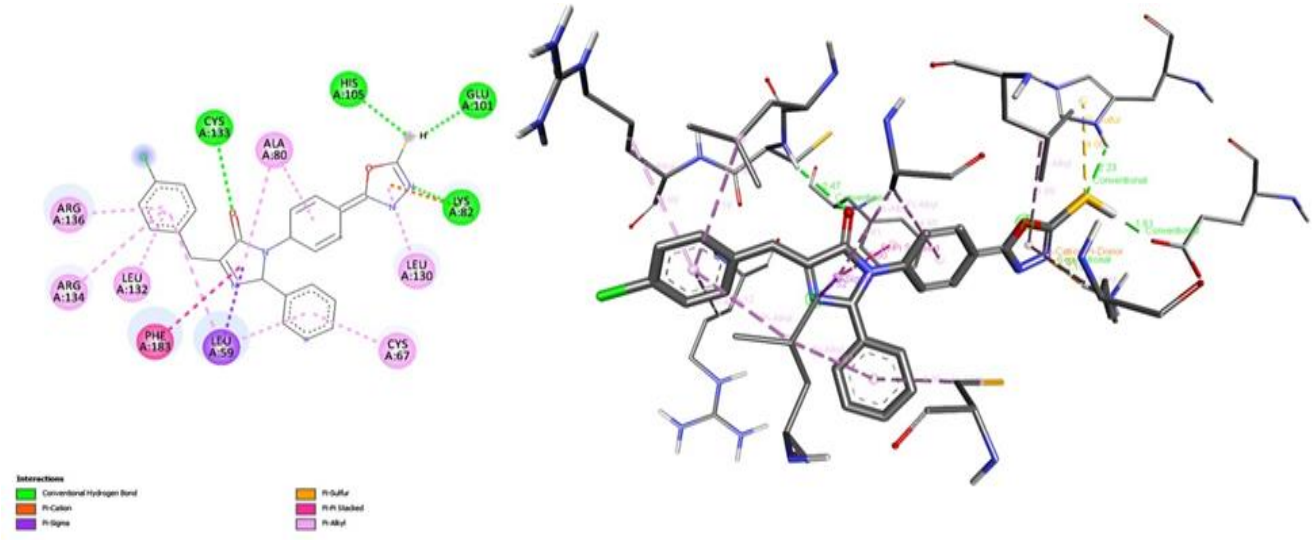

Figure 9: 2D and 3D representation of complex 2d

Analysis of molecular docking

Docking analysis was run on compounds containing derivatives of novel 5-oxo-imidazolines with the protein target Polo-like kinase 1 (PKL1) in complex with B12356. For these studies, seven compounds with high pIC_{50} were chosen, and of those 7, compounds 2e, 2f and 2d had the highest docking scores, with values of 11.33, 11.12 and 10.95 kcal/mol, respectively (see Table 7).

Compound 2e displayed backbone conventional hydrogen bonding interactions with the imidazolidinone group with CYS 133 (2.37A^0), 5-mercapto-1,3,4 oxadiazole group with HIS 105 (2.11A^0), and GLU 101 (1.86 A^0). It also exhibited electrostatic pi-orbital cation, pi-donor hydrogen bond interactions with LYS 82 (2.50A^0), and hydrophobic pi-sigma interactions with amino acids. Moreover, the substance established a Pi-Alkyl hydrophobic connection with two LEU 130 amino acids at a distance of 5.46A^0, 4.95A^0, two amino acids of LEU 59 at a distance of 4.83A^0, 5.11A^0, and also Pi-Alkyl hydrophobic interactions with ALA 80 (4.31A^0), LYS 82 (5.20A^0), CYS 67 (4.15A^0), LEU 132 (5.02A^0), ARG 134 (4.86A^0), and ARG 136 (4.66A^0).

Another instance of backbone conventional hydrogen bonding contact between the imidazolidinone group and CYS 133(2.20A^0) was seen in compound 2f, 5- mercapto-1,3,4 oxadiazole group with ARG 134 (1.93A^0) and 4-methoxy benzylidene group with ASP 194 (1.75A^0), which is also having an electrostatic pi-orbital cation interaction with ARG 57 (4.08A^0), hydrophobic pi-sigma interaction with the amino acid LEU 59 (3.59A^0) and LUE 90 (3.31A^0), Pi-Pi stacked hydrophobic interaction with PHE183 (4.42A^0). Delocalized electrons in the pi-orbital of the benzene ring produced hydrophobic interactions with the alkyl groups of two amino acids of ALA 80 at a distance of (4.27A^0), (5.15A^0), LEU 59 (4.25A^0), (5.13A^0), ARG 136 (4.21A^0), (4.48A^0), HIS 105 (4.25A^0), and VLA 114 (4.72A^0) in the molecule.

Compound 2d showed four conventional hydrogen bonding interactions between the imidazolidinone group with CYS 133 (2.46A^0), 5-mercapto-1,3,4 oxadiazole group with HIS 105 (2.22A^0), and GLU 101 (1.87 A^0) which is having an electrostatic pi-orbital cation and pi-donor hydrogen bond interaction with LYS 82 (2.53A^0). Hydrophobic pi-sigma interaction with the amino acid LEU 59 (3.51A^0), Pi-Pi stacked hydrophobic interaction with PHE183 (5.60A^0), HIS 105 (4.06A^0) possess Pi-sulfur interaction, and ten amino acids demonstrated Pi-alkyl hydrophobic interaction. Furthermore, the compound formed a Pi-Alkyl hydrophobic bond with two amino acids of ALA 80 at a distance of 4.41A^0, 4.95A^0, and then with two amino acids of LEU 59 at a distance of 4.83A^0, 5.11A^0, and also Pi-alkyl hydrophobic interactions with CYS 67 (4.35A^0), LYS 82 (5.20A^0), LEU 130 (4.97A0), LEU 132 (5.19A^0), ARG 134 (4.98A^0), and ARG 136

(4.58A^0). Both the hydrogen bond and the hydrophobic interactions in the complexes showed that ligands 2e, 2f and 2d of 4-(5-mercapto-1, 3, 4-oxadiazolyl) 5-oxo-imidazoline derivatives are most active against Polo-like kinase 1(PKL1) in complex with B12356, respectively.

Conclusion

In this QSAR study, the original dataset was represented using descriptors, which resulted in a robust, stable, and predictive model. The establishment of a good statistical model has opened up a new avenue for studying descriptors in the suppression of *Polo-like kinase 1 (PKL1).* Internally and externally, the model is validated using software statistical parameters. To predict bioactivity, the model is tested on designed substances. To aid our QSAR model, we performed molecular docking studies on the best-predicted active chemicals to obtain structural and interaction information. Compounds 2e, 2f, and 2d obtained the highest docking scores, with scores of -11.33, -11.12, and -10.95 kcal/mol, to design and manufacture innovative estrogen-positive (MCF-7 cell line) breast cancer treatments, these compounds would serve as the most potent (PKL1) inhibitors, demonstrating a medical revolution. The pharmacokinetics analysis (drug-likeness test) performed on the designed molecules also showed that all compounds can advance to the next pre-clinical trial stage because they passed the drug-friendliness examination (ADME and other physicochemical properties) and because they complied with the Rule of Five, a benchmark used to evaluate the drug-likeness of compounds. The use of the MCF-7 cell line represents a significant step forward in the search for a permanent cure for breast cancer.

Acknowledgements

The authors would like to thank the Management of SRM College of Pharmacy for their support and encouragement and Dr. Paolo Gramatica, QSAR Research Unit, Insubria University, Italy, for the academic licensing software.

Conflict of interest

The Authors declared no conflict of interest in this article.

Authors' Contributions

All authors contributed to data analysis, drafting, and revising of the paper and agreed to be responsible for all the aspects of this work.

Funding

No funding was received to assist with the preparation of this article.

Ethical approval

There is no ethical approval in this article.

ORCID

Yellasubbaiah N

https://orcid.org/0000-0001-7109-6992
Velmurugan V
https://orcid.org/0000-0001-5316-6854

References

[1]. Bajaj S., Roy P.P., Singh J., Synthesis, thymidine phosphorylase inhibitory, and computational study of novel 1, 3, 4-oxadiazole 2-thione derivatives as potential anticancer agents, *Computational Biology and Chemistry,* 2018, **76**:151 [Crossref], [Google Scholar], [Publisher]
[2]. Bhaumik I., Pal K., Debnath U., Karmakar P., Jana K., Misra A.K., Natural products inspired allicin analogs as novel anti-cancer agents, *Bioorganic Chemistry*, 2019, **86**:259 [Crossref], [Google Scholar], [Publisher]
[3]. Sung H., Ferlay J., Siegel R.L., Laversanne M., Soerjomataram I., Jemal A., Global cancer statistics 2020: GLOBOCAN estimates of incidence and mortality worldwide for 36 cancers in 185 countries, *CA: a cancer journal for clinicians,* 2021, **71**:209 [Crossref], [Google Scholar], [Publisher]
[4]. Anderson B.O., Ilbawi A.M., Fidarova E., Weiderpass E., Stevens L., Abdel-Wahab M., Mikkelsen B., The Global Breast Cancer Initiative: a strategic collaboration to strengthen health care for non-communicable diseases, *The Lancet*

Oncology, 2021, **22**:578 [Crossref], [Google Scholar], [Publisher]
[5]. Liu L., Tang Z., Wu C., Li X., Huang A., Lu X., You Q., Xiang H., Synthesis and biological evaluation of 4, 6-diaryl-2-pyrimidinamine derivatives as anti-breast cancer agents, *Bioorganic & Medicinal Chemistry Letters,* 2018, **28**:1138 [Crossref], [Google Scholar], [Publisher]
[6]. Jordan V.C., Brodie A.M., Development and evolution of therapies targeted to the estrogen receptor for the treatment and prevention of breast cancer, *Steroids*, 2007, **72**:7 [Crossref], [Google Scholar], [Publisher]
[7]. De Cárcer G., The mitotic cancer target polo-like kinase 1: oncogene or tumor suppressor? *Genes*, 2019, **10**:208 [Crossref], [Google Scholar], [Publisher]
[8]. Sanhaji M., Kreis N.N., Zimmer B., Berg T., Louwen F., Yuan J., p53 is not directly relevant to the response of polo-like kinase 1 inhibitors, *Cell Cycle*, 2012, **11**:543 [Crossref], [Google Scholar], [Publisher]
[9]. Abo-Elanwar Y.A., Mostafa A.S., El-Sayed M.A., Nasr M.N., Synthesis and biological evaluation of new 2-(4-fluorophenyl) imidazol-5-ones as anticancer agents, *Journal of Applied Pharmaceutical Science,* 2019, **9**:001 [Crossref], [Google Scholar], [Publisher]
[10]. Zhang C., Li Q., Meng L., Ren Y., Design of novel dopamine D2 and serotonin 5-HT2A receptors dual antagonists toward schizophrenia: an integrated study with QSAR, molecular docking, virtual screening, and molecular dynamics simulations, *Journal of Biomolecular Structure and Dynamics*, 2020 **38**:860 [Crossref], [Google Scholar], [Publisher]
[11]. Premakumari C., Muralikrishna A., Padmaja A., Padmavathi V., Park S.J., Kim T.J., Reddy G.D., Synthesis, antimicrobial and anticancer activities of amidosulfonamido methane linked bis heterocycles, *Arabian Journal of Chemistry,* 2014, **7**:385 [Crossref], [Google Scholar], [Publisher]
[12]. Iqbal J., Ejaz S.A., Khan I., Ausekle E., Miliutina M., Langer P., Exploration of quinolone and quinoline derivatives as potential anticancer agents, *DARU Journal of Pharmaceutical Sciences,* 2019, **27**:613 [Crossref], [Google Scholar], [Publisher]
[13]. Abdullahi M., Uzairu A., Shallangwa G.A., Mamza P., Arthur D.E., Ibrahim M.T., In-silico modeling studies on some C14-urea-tetrandrine derivatives as potent anti-cancer agents against prostate (PC3) cell line, *Journal of King Saud University-Science,* 2020, **32**:770 [Crossref], [Google Scholar], [Publisher]
[14]. Ibrahim M.T., Uzairu A., Shallangwa G.A., Ibrahim A. In-silico studies of some oxadiazoles derivatives as anti-diabetic compounds, *Journal of King Saud University-Science,* 2020, **32**:423 [Crossref], [Google Scholar], [Publisher]
[15]. Abdulrahman H.L., Uzairu A., Uba S., Insilico studies of some 2- anilinopyrimidine derivatives as anti-triple-negative breast cancer agents, *Beni-Suef University Journal of Basic and Applied Sciences,* 2020, **9**:13 [Crossref], [Google Scholar], [Publisher]
[16]. Kennard R.W., Stone L.A., Computer-aided design of experiments, *Technometrics*, 1969, **11**:137 [Crossref], [Google Scholar], [Publisher]
[17]. Tropsha A., Gramatica P., Gombar V.K., The importance of being earnest: validation is the absolute essential for successful application and interpretation of QSPR models, *QSAR & Combinatorial Science,* 2003, **22**:69 [Crossref], [Google Scholar], [Publisher]
[18]. Said M.F., George R.F., Petreni A., Supuran C.T., Mohamed N.M., Synthesis molecular modelling and QSAR study of new N-phenylacetamide-2-oxoindole benzenesulfonamide conjugates as carbonic anhydrase inhibitors with antiproliferative activity, *Journal of Enzyme Inhibition and Medicinal Chemistry,* 2022, **37**:701 [Crossref], [Google Scholar], [Publisher]
[19]. Dong J., Cao D.S., Miao H.Y., Liu S., Deng B.C., Yun Y.H., Wang N.N., Lu A.P., Zeng W.B., Chen A.F., Chem Des an integrated web-based platform for molecular descriptor and fingerprint computation, *Journal of cheminformatics*, 2015, **7**:60 [Crossref], [Google Scholar], [Publisher]
[20]. Cotuá V.J., Llinás S.H., Cotes O.S., Virtual Screening Based on QSAR and Molecular Docking of Possible Inhibitors Targeting Chagas CYP51, *Journal of Chemistry*, 2021, **2021**:6640624 [Crossref], [Google Scholar], [Publisher]
[21]. Alomari F.Y., Sharfalddin A.A., Abdellattif M.H., Domyati D., Basaleh A.S., Hussien M.A.,

QSAR Modeling, Molecular Docking and Cytotoxic Evaluation for Novel Oxidovanadium (IV) Complexes as Colon Anticancer Agents, *Molecules* 2022, **27**:649 [Crossref], [Google Scholar], [Publisher]

[22]. Wang X., Duan W., Lin G., Li B., Chen M., Lei F., Synthesis 3D-QSAR and Molecular Docking Study of Nopol-Based 1, 2, 4-Triazole-Thioether Compounds as Potential Antifungal Agents, *Frontiers in Chemistry,* 2021, **9**:757584 [Crossref], [Google Scholar], [Publisher]

[23]. Mishra S., Dahima R., In vitro ADME studies of TUG-891, a GPR-120 inhibitor using SWISS ADME predictor, *Journal of drug delivery and therapeutics,* 2019, **9**:36 [Crossref], [Google Scholar], [Publisher]

[24]. Abdulfatai U., Uzairu A., Uba S., Molecular docking and quantitative structure-activity relationship study of anticonvulsant activity of aminobenzothiazole derivatives, *Beni-Suef University Journal of Basic and Applied Sciences,* 2018, **7**:204 [Crossref], [Google Scholar], [Publisher]

[25]. Di Tullio M., Maccallini C., Ammazzalorso A., Giampietro L., Amoroso R., De Filippis B., Fantacuzzi M., Wiczling P., Kaliszan R., QSAR, QSPR and QSRR in terms of 3-D-MoRSE descriptors for in silico screening of clofibric acid analogues, *Molecular Informatics,* 2012, **31**:453 [Crossref], [Google Scholar], [Publisher]

HOW TO CITE THIS ARTICLE

Yellasubbaiah N, Velmurugan V. QSAR Modeling, Molecular Docking, and ADME Studies of Novel 5-Oxo- Imidazoline Derivatives as Anti-Breast Cancer Drug Compounds against MCF-7 Cell Line. *J. Med. Chem. Sci*., 2023, 6(12) 3087-3112.
DOI: https://doi.org/10.26655/JMCHEMSCI.2023.12.24
URL: https://www.jmchemsci.com/article_177388.html